RAPID COMMUNICATION

Bismuth-content-dependent polarized Raman spectrum of InPBi alloy*

Guan-Nan Wei(魏冠男)[1], Qing-Hai Tan(谭青海)[1], Xing Dai(戴兴)[1], Qi Feng(冯琦)[1], Wen-Gang Luo(骆文刚)[1], Yu Sheng(盛宇)[1], Kai Wang(王凯)[2], Wen-Wu Pan(潘文武)[2], Li-Yao Zhang(张立瑶)[2], Shu-Min Wang(王庶民)[2], and Kai-You Wang(王开友)[1,†]

[1] *State Key Laboratory of Superlattices and Microstructures, Institute of Semiconductors, Chinese Academy of Sciences, Beijing* 100083, *China*

[2] *State Key Laboratory of Functional Materials for Informatics, Shanghai Institute of Microsystem and Information Technology, Chinese Academy of Sciences, Shanghai* 200050, *China*

(Received 28 January 2016; revised manuscript received 7 March 2016; published online 25 May 2016)

We systematically investigate the optical properties of the $InP_{1-x}Bi_x$ ternary alloys with $0 \leq x \leq 2.46\%$, by using high resolution polarized Raman scattering measurement. Both InP-like and InBi-like optical vibration modes (LO) are identified in all the samples, suggesting that most of the Bi-atoms are incorporated into the lattice sites to substitute P-atoms. And the intensity of the InBi-like Raman mode is positively proportional to the Bi-content. Linear red-shift of the InP-like longitudinal optical vibration mode is observed to be 1.1 cm^{-1}/Bi%, while that of the InP-like optical vibration overtone (2LO) is nearly doubled. In addition, through comparing the $Z(XX)\bar{Z}$ and $Z(XY)\bar{Z}$ Raman spectra, longitudinal-optical-plasmon-coupled (LOPC) modes are identified in all the samples, and their intensities are found to be proportional to the electron concentrations.

Keywords: InPBi, Raman spectra, red-shift, LOPC modes

PACS: 63.20.–e, 63.20.kd, 63.20.dd **DOI:** 10.1088/1674-1056/25/6/066301

1. Introduction

The temperature-insensitive semiconductor laser is one of the future key devices in the field of optical communications.[1,2] Bismuth-diluted alloys are expected to have temperature-insensitive band gaps,[3,4] and therefore are the promising candidates for the application in the optoelectronic devices. Berding *et al.* theoretically predicted that InPBi is the best potential candidate for mid- and far-infrared (IR) optoelectronic applications in InSbBi, InAsBi, and InPBi.[5] Thus isoelectronic Bi-doped InP has become an important topic in the search for a new semiconducting material. However, the InPBi alloy is the most difficult to mix, and until recently, have the $InP_{1-x}Bi_x$ materials been successfully grown by the gas source molecular beam epitaxy (GSMBE) technique.[2]

Raman scattering study is a very powerful technique to study the crystal quality and the associated vibration properties.[6] The vibration properties of the InPBi materials have been studied by using un-polarized Raman scattering measurement, where the InBi-like optical vibration modes were identified with Raman frequencies of 148 and 170 cm^{-1}.[7,8] Yet in the previous work those Bi-induced modes were not subtracted from the background signals provided by the InP-like acoustical vibration modes. And the longitudinal-optical-plasmon-coupled (LOPC) modes have not been identified, nor have the shifts of the InP-like optical modes. Unlike the previous work, here we use polarized micro-Raman scattering system with much higher resolution to further investigate the Bi-content dependent vibration properties of the $InP_{1-x}Bi_x$ alloys with $0 \leq x \leq 2.46\%$. To compare the Raman spectra under different polarized conditions, we are able to assign the InBi-like Raman features at about 148 cm^{-1} and 170 cm^{-1} to out-of-plane and in-plane vibration modes, respectively. Intensities of the InBi-like optical vibration modes are found to increase with increasing the Bi-content. Linear red-shift of the InP-like longitudinal optical vibration mode is observed to be 1.1 cm^{-1}/Bi%, while that of InP-like optical vibration overtone (2LO) is nearly doubled. In addition, the occurrence of LOPC mode is verified by comparing two polarized Raman spectra, and the Bi-content dependent LOPC intensity and the free-electron concentration have the same variation trend.

2. Experiment

2.1. Sample details

The about 400-nm thick $InP_{1-x}Bi_x$ films were grown on (100) semi-insulating InP substrates by V90 gas source

*Project supported by the National Basic Research Program of China (Grant No. 2014CB643903) and the National Natural Science Foundation of China (Grant Nos. 61225021, 11474272, and 11174272).

†Corresponding author. E-mail: kywang@semi.ac.cn

© 2016 Chinese Physical Society and IOP Publishing Ltd

molecular beam epitaxy (GSMBE) at a typical growth temperature of around 320 °C. Bi compositions of the samples were determined by employing high resolution x-ray diffraction (HRXRD) ω–2θ scans on two asymmetric (115) and two symmetric (004) planes and an InBi lattice constant of 6.52 Å. In the growth process, elemental In and Bi fluxes were controlled by adjusting the respective effusion cell temperature while P_2 was cracked from PH_3 at 1000 °C. The Bi content was just controlled by varying Bi cell temperature. The growth rate was 800 nm/h and the PH_3 pressure was set to be 350 Torr (1 Torr = 1.33322×10^2 Pa) for the samples with Bi content $< 2.2\%$. A larger PH_3 pressure of 400 Torr was used for the sample with Bi content of 2.46%. The epilayers were cut into pieces each with a size of 1-cm square for Raman scattering measurements, with mirror-like surface.

2.2. Raman setup

Raman spectrum measurements were performed in a backscattering geometry using a Jobin-Yvon HR800 Raman system equipped with a liquid nitrogen cooled charge-coupled detector. The excitation wavelength was 632 nm from a diode-pumped solid-state laser. A power of 0.5 mW was used for excitation. The scattered light was analyzed by a triple monochromator (Dilor XY) equipped with aliquid-nitrogen-cooled CCD array. Using a high precision microscope, the laser spot size could be focused into a spot with around 1 μm in diameter, which enables us to investigate the spatial homogeneity of the sample. A 2400 g/mm diffraction grating (with $\sim$0.2 cm^{-1}) was used. Correct instrument calibration was verified by checking the position of the Si band at $\pm$520.7 cm^{-1}. The widely used Porto notations $Z(XX)\bar{Z}$ and $Z(XY)\bar{Z}$ have been used for designating the crystal and polarization directions in this work.[9,10] The incident and scattered laser beams for both configurations are perpendicular to the sample surface. In the polarized Raman measurements, for $Z(XX)\bar{Z}$ configuration, polarization direction of the scattered light was parallel to the polarization of incident laser beam. However, in $Z(XY)\bar{Z}$ configuration, the polarization direction of the scattered light was perpendicular to that of the incident one. Because the thickness values of InPBi films were large compared with the optical absorption depth, the signal contribution from the substrate was negligible.

3. Results and discussion

Polarized Raman scattering studies allow us to further confirm the symmetry of the main Raman feature. Taking the $InP_{1-x}Bi_x$ alloys with $x = 1.47\%$ for example, figure 1 shows the Raman features obtained under both the $Z(XX)\bar{Z}$ configuration (red line (upper)) and $Z(XY)\bar{Z}$ configuration (black line (lower)). For Raman spectra under $Z(XX)\bar{Z}$ configuration, there are mainly six Raman features at 148, 170, 303, 311, 336, and 344 cm^{-1} marked as 1–6 between 80 cm^{-1} and 350 cm^{-1}. Raman peaks 2, 3, 5, and 6 also exist in Raman spectra under $Z(XX)\bar{Z}$ configuration, while peaks 1 and 4 are missing. Raman peaks 3–6 can be assigned to the InP-like Raman optical modes.[11,12] Accordingly, Raman peaks 3 and 4 can be assigned to InP-like transverse optical vibration modes at Γ point TO(Γ) and X point TO(X) respectively, while for Raman peaks 5 and 6, the InP-like longitudinal optical vibration modes at L point LO(L) or X point LO(X) and at Γ point LO(Γ), respectively. The sharp and strong InP-like Raman longitudinal optical vibration mode LO(Γ) (peak 6) indicates the existence of long range order of the InP structure in InPBi epilayer. The InP semiconductors with typical III–V group zinc-blende structures, show Td site symmetry. Unpolarized Raman spectra recorded from the InP (100) surfaces show the contributions of the three irreducible components Γ_1, Γ_{12}, and Γ_{15}.[11] Thus the Raman spectra in $Z(XX)\bar{Z}$ configuration containing $\Gamma_1 \oplus 4\Gamma_{12}$ symmetry, show the in-plane vibrational modes. While the Raman spectra in $Z(XY)\bar{Z}$ configuration with Γ_{15} symmetry show the out-of-plane vibration modes. This well explains why the Raman peaks 3, 5, and 6 should be allowed in the $Z(XX)\bar{Z}$ and $Z(XY)\bar{Z}$ Raman scattering geometries, while Raman peak 4 is missing in the $Z(XY)\bar{Z}$ configuration.

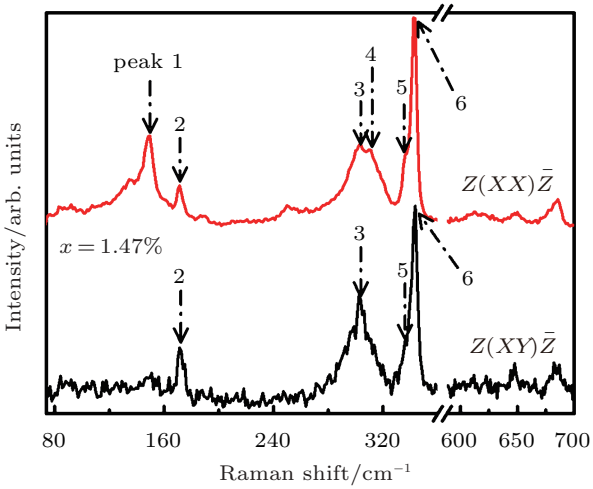


Fig. 1. (color online) Raman spectra for $InP_{1-x}Bi_x$ alloys with $x = 1.47\%$, under $Z(XX)\bar{Z}$ (red line (upper)) and $Z(XY)\bar{Z}$ (black line (lower)) configurations.

The Raman peaks 1 and 2 belonging to the InBi-like optical vibration modes[7] can be assigned to Raman optical modes TO and LO. The InBi mode in $InP_{1-x}Bi_x$ should originate from the substitutional Bi atoms at the P site, resulting in the same Raman selection rules for both InBi and InP modes. Therefore, the Raman selection rules in the $Z(XX)\bar{Z}$ and $Z(XY)\bar{Z}$ scattering geometries for the InBi mode in $InP_{1-x}Bi_x$ alloys.[13] The optical phonon frequency of InBi mode can be estimated from the equation: $\omega_{InBi} = \omega_{InP} \cdot \sqrt{\mu_{InP}/\mu_{InBi}}$, where μ_{InP} and μ_{InBi} are the reduced mass of In–P and In–Bi, respectively.[14] Considering that the TO (peak 4) and LO

(peak 6) phonon frequencies of InP, the InBi mode is expected to be near the spectral range between 150 cm^{-1} and 200 cm^{-1}. This can also well explain why the peaks 1 and 4 both are missing in the $Z(XY)\bar{Z}$ Raman scattering geometry.

With many more Raman features appearing in Raman spectra for the $Z(XX)\bar{Z}$ configuration, we present in Fig. 2 the Bi-content-dependent $Z(XX)\bar{Z}$ polarized Raman spectra for the series of $InP_{1-x}Bi_x$ alloys with $0 \le x \le 2.46\%$. In order to better analyze the spectra, the Raman features are marked as three different regions, I (low-frequency region), II (medium-frequency region), and III (high-frequency region), respectively. In the following, we will discuss the sections with Bi-composition dependent Raman features in details one by one.

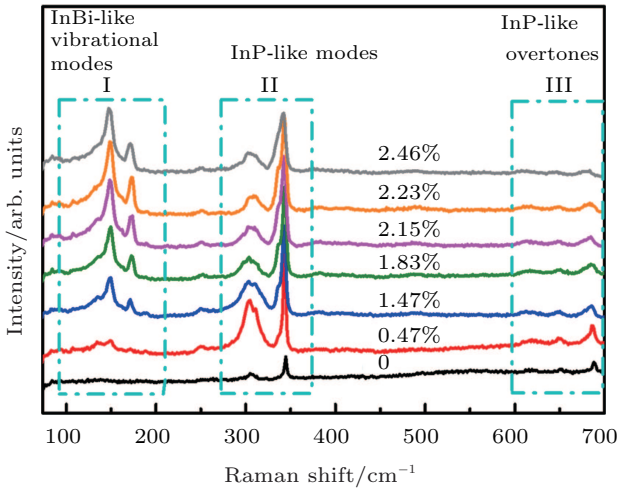


Fig. 2. (color online) Raman spectra under $Z(XX)\bar{Z}$ configurations for $InP_{1-x}Bi_x$ samples, with $0 \le x \le 2.46\%$, in the range from 75 cm^{-1} to 700 cm^{-1}. InBi-like optical vibration modes are observed in the low-frequency region (marked I). InP-like optical vibration modes are observed in the medium frequency region (marked II), while InP-like optical vibration overtones are observed in the high frequency region (marked III).

The low frequency region Raman spectra for the $InP_{1-x}Bi_x$ alloys with are shown in Fig. 3(a). In order to see the weak peaks clearly, the intensities of the Raman spectra are multiplied by 15, 3, and 1.5 for $x = 0$, 0.47%, and 1.47% samples, respectively. High resolution techniques allow us to identify those weaker background signals as Raman features at about 117, 135, 154, 162, and 188 cm^{-1}, which also appear in the InP reference samples. Those five weaker Raman features are assigned to the InP-like transverse or longitudinal acoustical modes and their overtones, 2LA(L), 2TA(K), LA(W), LA(L), 2TA(W).[11,12] With adding the Bi atoms into the InP crystal, two extra peaks at 148.5 cm^{-1} and 171.5 cm^{-1} are observed, where the first one is assigned to InBi-like TO mode and the second one to LO mode.[7] The Raman peak intensities for both the InBi-like TO and LO modes increase with increasing the Bi doping level, while the peak positions for these two modes are not sensitive to the Bi doping concentration. In order to characterize the Bi-content dependent intensities and peak-site behaviors of the InBi-like Raman features, we need to rule out the background scattering features, where the peak positions for the background signals should be not sensitive to the variation of the Bi composition. The Raman spectra for all the Bi doped samples can be well fitted by considering the InP background signals and the InBi-like modes, which are shown in Fig. 3(a). The intensity ratio between the InBi-like TO and LO modes R_{Bi} ($R_{Bi} = [I(x) - I(0.47\%)]/I(0.47\%)$, versus Bi content% of $InP_{1-x}Bi_x$ sample is shown in Fig. 3(b). The intensity ratio for both the InBi-like TO and LO modes linearly increases with increasing the Bi content, where the relation between R_{Bi} and Bi content (x) is $R_{Bi} \sim x$, with a fitting slope value of 4.78 per Bi%. It is worth noting that Bi content dependent R_{Bi} relations for both the InBi-like TO and LO modes possess the same variation trend with Bi content%, indicating that these two modes are closely linked with increasing the Bi doping.

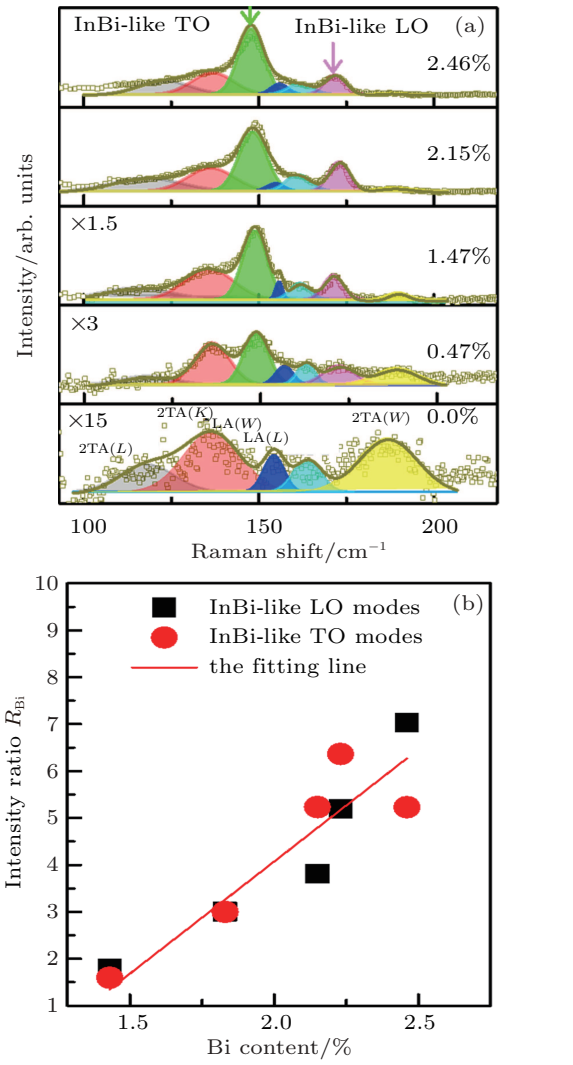


Fig. 3. (color online) (a) InBi-like vibration modes TO (represented by the red section) and LO (purple section), together with InP-like disorder-activated acoustical modes, which are used for the multi-peak fitting in the low frequency range from 93 cm^{-1} to 218 cm^{-1}. The intensities of the Raman spectra are multiplied by 15, 3, and 1.5 for $x = 0$, 0.47%, and 1.47% samples, respectively. (b) The Bi content dependent TO (red solid) and LO (black square) intensity ratio R_{Bi} ($R_{Bi} = [I(x) - I(0.47\%)]/I(0.47\%)$) for the $InP_{1-x}Bi_x$ sample, and the solid line is for the fitted results.

Figure 4 shows the analysis of the Bi content dependent Raman spectra in the medium frequency region. Three different kinds of Raman features need to be introduced to fit the Raman spectra between 270 cm^{-1} and 330 cm^{-1}, which are InP-like transverse optical vibration modes TO(Γ) (green peak), TO(X) (purple peak), and LOPC mode (red peak) as shown in Fig. 4(a). The reason is that if only Raman features of TO(Γ) and TO(L) exist in the Raman spectra under $Z(XX)\bar{Z}$ configuration, then consequently there will be only TO(Γ) left in the Raman features under $Z(XY)\bar{Z}$ configuration. However, as shown in Fig. 4(b), the peak TO(L) does go missing under $Z(XY)\bar{Z}$ configuration, yet the width of the Raman curve keeps the same. So there must exist another Raman feature. Then, we will show that most likely the LOPC mode is a candidate. In a polar semiconductor, the free-carrier Plasmon and the longitudinal-optical (LO) phonons are coupled by the interaction between the electric dipole moment due to the relative displacement of the ions and the electric field associated with the free carriers.[15] In that case, these modes will appear near the LO phonon frequency, also named LO-phonon-plasmon coupled (LOPC) mode. Commonly, there are two coupled modes in heavily doped n-type InP material,[16] i.e., the upper (L^+) and lower (L^-) longitudinal branches of the coupled plasmon-LO phonon modes. In InP with high electron concentration ($n \sim 10^{18}$ cm^{-3}), the frequency of the upper branch is much higher than the LO phonon frequency, while that of the lower branch is closely equal to the TO phonon frequency.[17,18] The electron concentrations of the InPBi materials are on the order of 10^{18} cm^{-3}, which were calculated through Hall transport measurements. Thus the lower (L^-) longitudinal branche of the coupled plasmon-LO phonon mode centered at about 303 cm^{-1} is introduced in the fitting procession.[18] After considering these three modes, the Raman spectra for different samples can be well fitted. For Raman spectra in the range between 330 cm^{-1} and 350 cm^{-1}, two kinds of Raman features, which are the InP-like LO(Γ) and LO(L) modes are introduced into the fitting progress as shown in Fig. 4(a). Because the intensity of the LOPC mode is strongly dependent on the carrier density, LOPC mode is often used as a nondestructive probe to investigate the relative doping level of the n-type semiconductors.[19,20] During the MBE growth, PH_3 pressure will affect the electron concentrations,[7] so figure 4(c) only shows the electron concentrations for samples with Bi composition $x \leq 2.23\%$, which have the same growth condition and PH3 pressure during the growth. Figure 4(c) shows that the ratio of I_{LOPC}/I_{LO} does not vary linearly with Bi doping concentration increasing, but has a similar trend to the electron densities obtained from Hall Effect measurements. This proves that the I_{LOPC} indeed can be used as a rapid and sensitive method to determine the relative doping level in n-type semiconductor. The non-linear behavior of the Bi composition-dependent electron concentration will be further discussed in our future work.

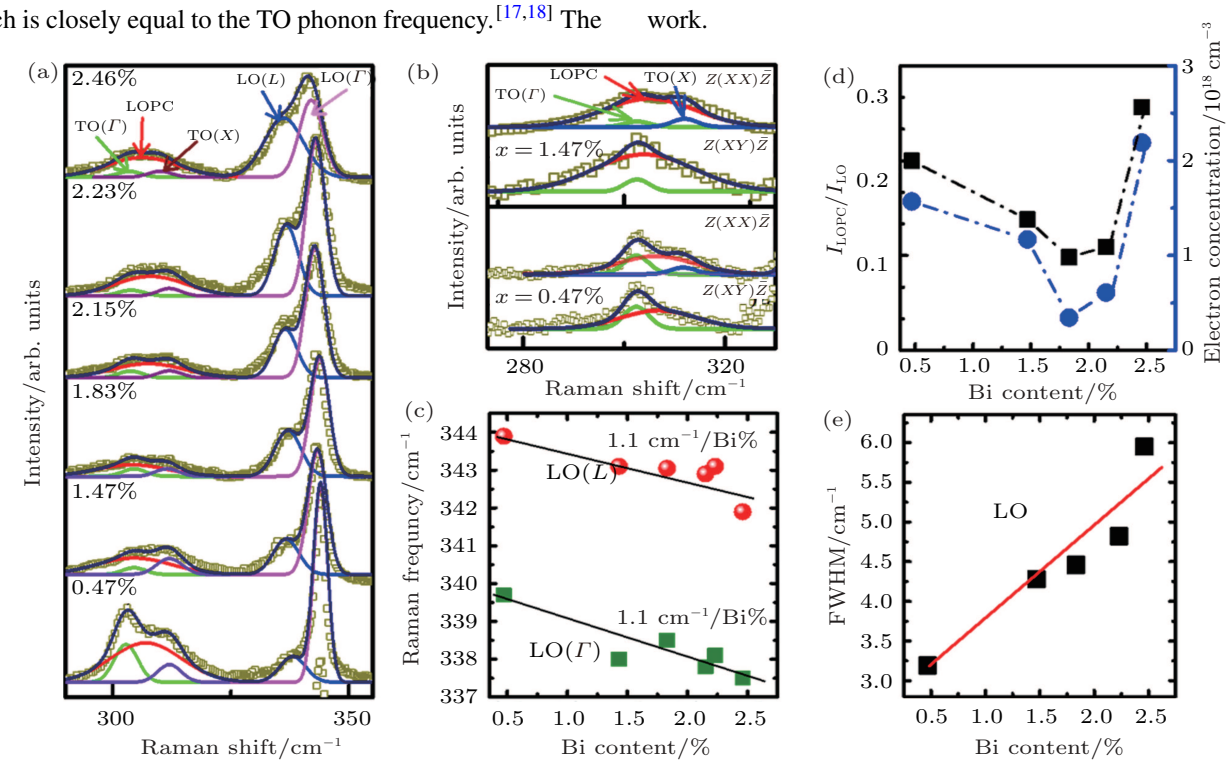


Fig. 4. (color online) (a) Raman spectra between 280 cm^{-1} and 365 cm^{-1} with different Bi doping levels, where the dark yellow dots are the experimental data. InP-like TO(L) (green line), LOPC (red line), and TO(Γ) (purple line) modes are used to fit the spectra between 280 cm^{-1} and 325 cm^{-1}, and LO(L) (blue line) and LO(Γ) (magneta line) modes are used to fit the spectra between 325 cm^{-1} and 365 cm^{-1}. Navy lines are the fitted curves. (b) Comparison of the Raman spectra in the range from 270 cm^{-1} to 330 cm^{-1} between the $Z(XX)\bar{Z}$ and $Z(XY)\bar{Z}$ polarized configurations, for samples with $x = 0.47\%$ and 1.47%. (c) Bi content-dependent intensities of the LOPC and the corresponding electron concentrations for samples with Bi composition $x \leq 2.23\%$. (d) The Bi doping content-dependent shifts of the Raman frequencies of LO(L) and LO(Γ) modes. (e) The Bi composition-dependent full width at half maximum (FWHM) of LO(Γ). The black dots represent the experimental data, while the red line guides the eye.

Red shifts for both of the LO(Γ) and LO(L) modes linearly increase with increasing the Bi doping level, which is shown in Fig. 4(d). The red shifts of the Raman frequency for both of the InP-like LO(Γ) and LO(L) modes are both to be 1.1 cm^{-1}/Bi%. This may lie in the enlargement of lattice constant, which varies linearly from 5.86 Å to 5.88 Å[5] with x increasing from 0 to 2.46%. The intense and narrow LO peak is indicative of the long-range order of the InP-host crystal. Figure 4(e) shows the Bi composition-dependent FWHM of the $InP_{1-x}Bi_x$ sample. With increasing the Bi doping level, the FWHM nearly increases linearly from ~3.2 cm^{-1} (at $x = 0.47\%$) to 5.9 cm^{-1} (at $x = 2.46\%$). The increase of the FWHM suggests that the quality of the InPBi crystal is slowly away from the perfect Td symmetry with increasing the Bi-content.

Finally, in the high frequency region (region III), strong second order spectrum between 600 cm^{-1} and 700 cm^{-1} is observed. As have been confirmed by other researchers, Raman structures at 615, 649, and 683 cm^{-1} are attributed to a combined creation of LO and TO phonons at various critical points,[21] which are the 2TO, TO + LO, and 2LO phonons at Γ point, L point or X point. Raman frequencies of both the 2LO and TO + LO decrease with Bi-content increasing, while that of 2TO is insensitive to the Bi composition as shown in Fig. 5(b). The Red shift of the 2LO is around 2.83 cm^{-1} per Bi%, which is about twice that of LO. And the red shift of the TO + LO (1.32 cm^{-1} per Bi%) is almost equal to that of the LO. Moreover, the width of the combination band TO + LO (649 cm^{-1}) is smaller than those of the 2TO (615 cm^{-1}) and 2LO (683 cm^{-1}) overtones, indicating that the orderings of the phonon frequencies at Γ, L, and X for the TO and LO branches are the reverse of each other.[20] Owing to the facts that these second-order peaks are very sensitive to lattice symmetry, they can be used to monitor the degree of disorder in the samples.[21–23] As shown in Fig. 5(c), the FWHM of 2LO increases almost linearly as Bi composition increases, indicating that the distortion of the InPBi crystal increases with increasing the Bi doping concentration.

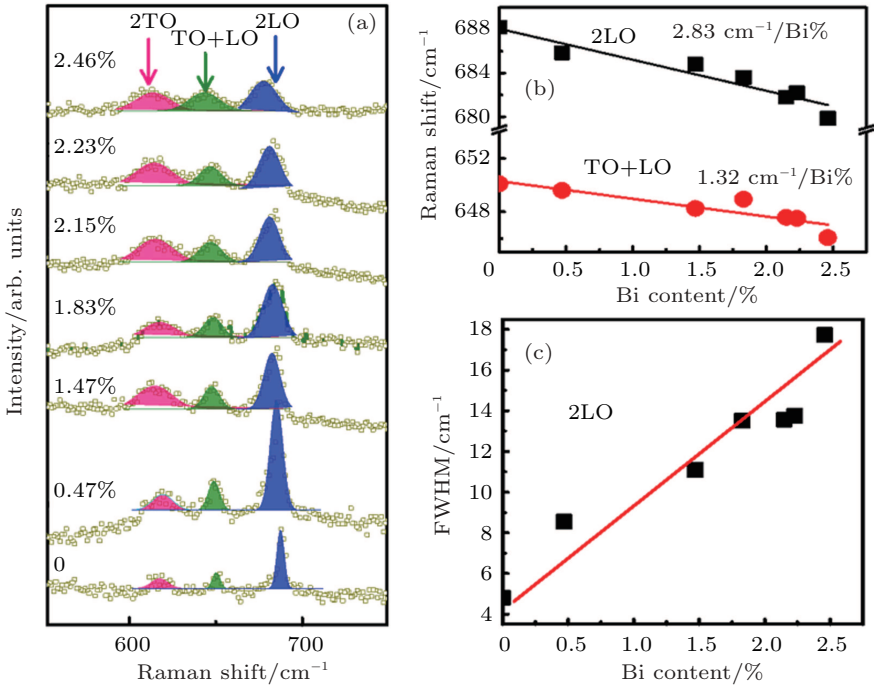


Fig. 5. (color online) (a) Infrared Raman spectra for a series of InPBi samples. The pink sections (2TO), the olive sections (TO + LO) and blue ones (2LO) represent the overtones of TO and LO. (b) The Bi doping level dependent Raman shifts of the 2LO and TO + LO. The dots represent the experimental data, while the straight lines represent the linear fitting progress. (c) The Bi doping level dependent FWHM of 2LO, where the dots represent the experimental data, and the line guides the eye.

4. Conclusions

In this work, we systematically investigate the vibration properties of the constituent alloys $InP_{1-x}Bi_x$ with $0 \leq x \leq 2.46\%$ by using the polarized high resolution micro-Raman. Both InP-like and InBi-like optical vibration modes (LO) are identified in all the samples, suggesting that most of the substitutional Bi-atoms are incorporated into the lattice sites to replace the P-atoms. The intensities of the InBi-like Raman modes increase linearly as Bi-content increasing. The red-shift of the Raman frequency of the InP-like longitudinal optical vibration mode is observed to be 1.1 cm^{-1}/Bi%, while that of InP-like optical vibration overtone (2LO) is more than doubled. The crystal distortion of the InP-host material is found to increase with increasing the Bi doping concentration. In addition, LOPC modes are identified by comparing the Raman spectra under $Z(XX)\bar{Z}$ and $Z(XY)\bar{Z}$ configurations. The Bi content-dependent intensity ratio between the LOPC and InP-like LO(Γ) mode has the same trend as the electron con-

centration, which can be used as a rapid and sensitive method to determine the relative doping level in n-type InPBi semiconductors.

References

[1] Gu Y, Wang K, Zhou H F, Li Y Y, Cao C F, Zhang L Y, Zhang Y G, Gong Q, and Wang S M 2014 *Nanoscale Res. Lett.* **9** 24

[2] Kondow M, Nakatsuka S, Kitatani T, Yazawa Y and Okai M 1996 *Jpn. J. Appl. Phys.* **35** 5711

[3] Svensson S P, Hier H, Sarney W L, Donetsky D, Wang D and Belenky G 2012 *J. Vac. Sci. Technol. B* **30** 02B109

[4] Song Y, Wang S, Roy I S, Shi P, Hallen A and Lai Z 2013 *J. Cryst. Growth* **378** 323

[5] Wang K, Gu Y, Zhou H F, Zhang L Y, Kang C Z, Wu M J, Pan W W, Lu P F, Gong Q and Wang S M 2013 *Sci. Rep.* **4** 5449

[6] Yue L, Wang P, Wang K, Wu X Y, Pan W W, Li Y Y, Song Y X, Gu Y, Gong Q, Wang S M, Ning J Q and Xu S J 2015 *Appl. Phys. Express* **8** 041201

[7] Pan W W, Steele J A, Wang P, Wang K, Song Y X, Yue L, Wu X Y, Xu H, Zhang Z P, Xu S J, Lu P F, Wu L Y, Gong Q and Wang S M 2015 *Semicond. Sci. Tech.* **30** 094003

[8] Das S C, Das T D and Dhar S 2012 *Infrared Phys. Technol.* **55** 306

[9] Zhang X, Han W P, Wu J B, Milana S, Lu Y, Li Q Q, Ferrari A C and Tan P H 2013 *Phys. Rev. B* **87** 115413

[10] Chen Y F, Dumcenco D O, Zhu Y M, Zhang X, Mao N N, Feng Q L, Zhang M, Zhang J, Tan P H, Huang Y H and Xie L M 2014 *Nanoscale* **6** 2833

[11] Bedel E, Landa G, Carles R, Redouls J P and Renucci J B 1986 *J. Phys. C: Solid State Phys.* **19** 1471

[12] Lin H H, Chung P K and Yen S T 2014 *Mater. Res. Express* **1** 045901

[13] Seong M J, Francoeur S, Yoon S, Mascarenhas A, Tixier S, damcyk M and Tiedje T 2005 *Superlattices Microstruct.* **37** 394

[14] Verma P, Oe K, Yamada M, Harima H, Herms M and Irmer G 2001 *J. Appl. Phys.* **89** 1657

[15] Yuasa T, Naritsuka S, Mannoh M, Shinozaki K, Yamanaka K, Nomura Y, Mihara M and Ishii M 1986 *Phys. Rev. B* **33** 1222

[16] Ernst S, Goi A R, Syassen K and Cardona M 1996 *Phys. Rev. B* **53** 1297

[17] Wan K and Young J F 1990 *Phys. Rev. B* **41** 10772

[18] Artús L, Cuscó R, Ibáñez J, Blanco N and González-Díaz G 1999 *Phys. Rev. B* **60** 5456

[19] Mlayah A, Carles R, Landa G, Bedel E and Muñoz-Yagüe A 1991 *J. Appl. Phys.* **69** 4064

[20] Steele J, Lewis R A, Henini M, Lemine O M and Fan D 2014 *Opt. Express* **22** 11680

[21] Artús L, Cuscó R, Martin J M and González-Díaz G 1994 *Phys. Rev. B* **50** 11552

[22] Ulrici B and Jahne E 1976 *Phys. Stat. Sol. (b)* **74** 601

[23] Yu S J, Asahi H, Emura S, Sumida H and Gonda S 1989 *J. Appl. Phys.* **66** 856